Soft Matter

Dynamic Article Links

Cite this: *Soft Matter*, 2012, **8**, 2924

www.rsc.org/softmatter

PAPER

Non-crystalline colloidal clusters in two dimensions: size distributions and shapes

Erez Janai,[a] Andrew B. Schofield[b] and Eli Sloutskin*[a]

Received 22nd September 2011, Accepted 20th December 2011
DOI: 10.1039/c2sm06808g

Cluster formation in many-body systems is very common, yet still not fully understood. We employ direct confocal microscopy to measure the size distribution and reconstruct the shapes of permanent gel clusters formed by sticky colloidal spheres in a two-dimensional (2D) suspension; the linear dimensions of the clusters are then measured by their radii of gyration R_g. We compare these non-ergodic clusters with the short-lived clusters, which reversibly form and deform, in a thermodynamically-equilibrated system of spherical colloids which interact solely by repulsions. Surprisingly, a similar behavior is observed for both types of clusters. In both cases, the average R_g of large clusters consisting of M particles scales as $\langle R_g \rangle \sim M^{1/2}$, which indicates that these clusters are solid, while the smaller clusters are much more ramified. A simple lattice model with a single free parameter quantitatively describes this complex behavior of $\langle R_g(M) \rangle$. The experimental size distribution $P(M)$ of our clusters is a (truncated) power law $M^{-\alpha}$, where the index α scales with colloid density and depends on the interparticle interactions. Strikingly, the observed behavior cannot be described by the common theoretical models which predict shorter correlation lengths and a density-independent value of α; thus, further theoretical efforts are necessary to fully understand the physics of clustering in this simple and fundamental system.

1. Introduction

During the previous decades, the collective behavior in many-body systems was among the most intensively studied areas of physics.[1] Yet even in the most trivial systems, such as the simple, non-interpenetrating disks on a plane, the collective behavior is still poorly understood. In particular, our understanding of particle self-organization into finite-sized clusters is still unsatisfactory.[2,3] In gels, these clusters are long-lived, determining the mechanical properties of the system.[4,5] In liquids, the self-organized clusters are short-lived, playing a dominant role in the physics of phase transitions[1] and glass formation.[6] The conventional experimental techniques are typically limited to yielding only two-body correlation functions;[7] thus, the size distribution of the n-particle clusters, determined by the n-body correlation functions, is usually experimentally inaccessible. Intermediate and long range correlations, which are abundant in many-body systems, increase the sensitivity to finite-size effects[1] which is a significant obstacle for computer simulations and dramatically limits the amount of information on clustering attainable by theoretical studies. As a result, the size and shape of particle clusters, which are among the most important characteristics of gels and fluids, are still unknown, even for the simplest and most fundamental systems.[4]

We employ confocal microscopy of colloids, micron-sized spherical particles in a solvent, to study the size distribution and the shape of microscopic clusters in a truly macroscopic, two-dimensional system.[8,9] Colloids are sufficiently small, such that they undergo Brownian motion; thus, their free energy tends to be minimized, and they exhibit crystallization[8] and melting,[9] mimicking atoms and molecules. The interactions between our colloids are tunable, from sticky to repulsive.[10–12] For sufficiently strong interparticle attractions, the colloids stick irreversibly, such that a gel[5] is formed. To quantify the shape of our clusters, we measure their radius of gyration R_g, which is the root mean square of the separation between the center of mass of a cluster and each of the particles belonging to the same cluster. We demonstrate that the variation of $\langle R_g \rangle$ with the cluster mass M, measured in particle mass units, is fully described by a simple theoretical model with only one free parameter. This parameter, the probability p for two particles to be next to each other, accounts for both the density of the particles and the interparticle interactions. Further, we demonstrate that the size distribution $P(M)$, which is the probability to find a cluster of mass M, follows a power law for both sticky and repulsive particles. Strikingly, the common theoretical models are unable to

[a]*Department of Physics and Institute for Nanotechnology and Advanced Materials, Bar-Ilan University, Ramat-Gan, 52900, Israel. E-mail: eli.sloutskin@biu.ac.il; Tel: +972 3738 4506*
[b]*The School of Physics and Astronomy, University of Edinburgh, Edinburgh, EH9 3JZ, UK*

reproduce this behavior of $P(M)$. Thus, even for this very simple and fundamental system, the full understanding of collective behavior is still missing.

2. Experimental details

To form our two-dimensional samples, we suspend PMMA [poly-(methylmethacrylate)] spheres, fluorescently-labelled for confocal imaging by the Nile Red dye, in dodecane (C_{12}, Sigma-Aldrich, ≥99%). The solution is then loaded into a rectangular Vitrocom capillary (0.1 × 2 × 50 mm) and sealed with epoxy glue. We pre-coat the capillary with PHSA [poly-(hydroxy-stearic) acid], which minimizes sticking of particles to the capillary walls. The particles sediment onto the bottom of the sample, forming a two-dimensional layer. The number density n of the particles in this layer is tunable, determined by the particles' concentration in the initial suspension. We determine the diameter of our particles by dynamic and static light scattering as $\sigma = 2.4$ μm; the size polydispersity of our particles is ≤5%. The density mismatch between PMMA and C_{12} is ~0.3 g cm^{-3}, such that the particles are effectively confined to move in two dimensions. The initial particles are sterically stabilized by PHSA, such that the van der Waals attractions are minimized[5] and the interparticle interactions are purely repulsive. When sticky interactions are to be introduced, we partially remove the PHSA monolayer from the surface of the particles by chemical etching in a mixture of sodium methoxide (Sigma-Aldrich, ≥99%). For a constant etching time of 30 min, the fraction of the PHSA monolayer removed[13] is determined by the concentration of sodium methoxide (4 ppm ≤ c ≤ 20 ppm) in the mixture.

To image our colloids, we employ the Nikon A1R confocal laser-scanning microscope in the resonant scanning mode, at 0.13 μm pixel^{-1}, which is close to the actual optical resolution.[14] Typically, the field of view in a single image is about 270 × 270 μm and ~30 static images, separated by 700 μm from each other, are taken across the sample in order to collect sufficient statistics, at ~24 h after the sample preparation. We repeat some of our measurements 3–4 days after the sample preparation; the results are unchanged, which indicates that the system reaches some type of an equilibrium state within several hours from the sample preparation. We detect the centers of all our particles within the two dimensional layer at the bottom of the sample, employing the PLuTARC image-analysis codes,[15] based on the algorithm of Crocker and Grier.[16] The area fraction of the particles in the image is obtained directly from the particle positions, as $\eta = n\pi\sigma^2/4$. We define clusters of particles based on the separation r between the centers of the particles in the confocal image. Particles separated by $r < r_c$ are considered connected, where $r_c = 1.25\sigma$, such that only the nearest-neighbor (NN) particles can match this criterion. The cut-off distance r_c was varied by up to 6% without changing any of the major results in our current work. According to this definition, for two particles to be considered connected, their surfaces do not necessarily have to be in a hard contact. A similar definition was employed in recent studies of electric conductivity in conductor–insulator composite materials, where the electrons move by tunneling over short distances between the surfaces of nearby conducting particles[17] and in recent computer studies of colloidal sedimentation.[2] Importantly, with this definition of clusters adopted, we do not distinguish between permanent clusters, which appear only in the presence of sticky interactions, and short-lived clusters, which appear at a sufficiently high particle density n in a static image of even a purely repulsive system.

3. Results and discussion

3.1 Radii of gyration: experimental results

To quantify the shape of the short-lived clusters, we measure the gyration radii R_g of clusters in a system of repulsive particles, where long-lived clusters do not form. For a cluster of M particles, the positions of which are given by a set of vectors $\{\vec{r}_i\}$, the radius of gyration is defined as $R_g = \left[M^{-1}\sum_i \left(\vec{r}_i - \overrightarrow{r_{CM}}\right)^2\right]^{1/2}$, where $\overrightarrow{r_{CM}} = M^{-1}\sum_i \vec{r}_i$ is the center of mass of the cluster and the summation is carried out over all M particles belonging to the cluster. The radii of gyration measure the linear dimensions of our clusters, which have, in general, complex ramified shapes, as shown in Fig. 1(a). Typically, for both solid and fractal objects in a two-dimensional space, the average $\langle R_g\rangle$ scales as $M^{1/d}$, where $d = 2$ for the solid objects; fractal objects are characterized by a smaller, fractal dimension. Interestingly, our experimental data does not follow a straight line when plotted on a log–log scale, as shown in Fig. 2(a). Instead, $\langle R_g\rangle \sim M^{1/2}$ only for the largest clusters (dashed, green line), which are, therefore, solid-like. For the smaller clusters, a different scaling is observed. This indicates that the small clusters are more ramified than the usual solid.

To test the universality of this behavior, we repeat the same measurement using sticky colloids ($\eta = 0.3$, $c = 20$ ppm), instead of the repulsive ones (see Fig. 1(b)). The sticky clusters are permanent and rigid, such that their shapes do not significantly change with time. Strikingly, in view of the distinct physical nature of these sticky clusters, the trends exhibited by their $\langle R_g(M)\rangle$ are similar to those observed above in the short-lived clusters, as shown in Fig. 2(b). As before, the scaling of the large clusters is $\langle R_g\rangle \sim M^{1/2}$, indicating that they are characterized by the dimension of their embedding space $d = 2$. The small clusters are more ramified, as was the case with the repulsive particles.

3.2 Radii of gyration: theoretical model

To quantitatively describe the $\langle R_g(M)\rangle$ of the smallest clusters, we compare them with the $\langle R_g(M)\rangle$ of lattice animals, random, connected clusters on a two-dimensional lattice.[18] The $\langle R_g(M)\rangle$

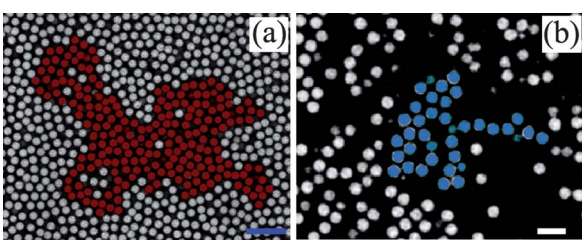

Fig. 1 (a) A raw confocal image of repulsive particles at $\eta = 0.49$, with one of the detected clusters overlaid in red. (b) The same for the sticky particles ($\eta = 0.3$, $c = 10$ ppm); the detected cluster is overlaid in blue. The bar lengths are 10 μm and 5 μm, in (a) and (b), respectively.

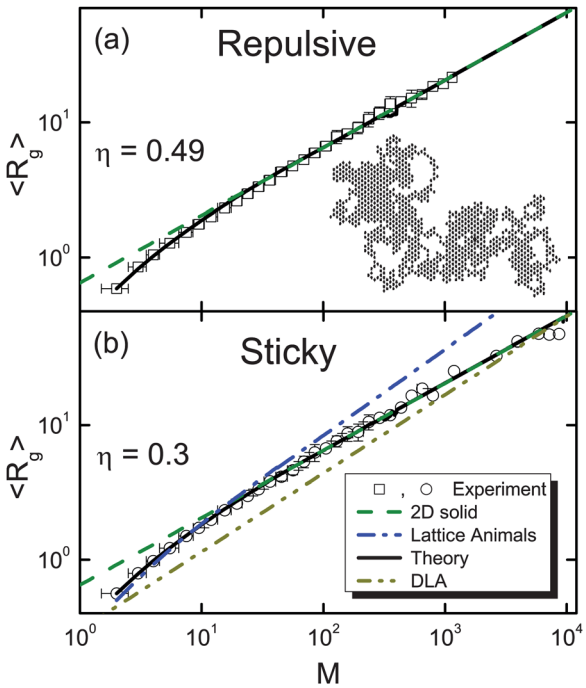

Fig. 2 The experimental average radii of gyration, in particle-diameter units, for systems of repulsive (a) and sticky (b) particles (open symbols) scale as $M^{1/2}$ for high M (dashed line), which is typical for solid, two-dimensional matter. The $\langle R_g \rangle$ of the smaller clusters exhibit a higher slope on this log–log scale, which indicates that the structure of these clusters is more ramified than a common two-dimensional solid. More precisely, these clusters are well-matched by $R_g(M)$ of the theoretical lattice animals (blue dash-dotted curve in (b)). Our theoretical model (solid curve) perfectly fits the experimental data for all M, for both the repulsive and the sticky particles. An example of a simulated lattice animal is shown in the inset to (a). The theoretical $\langle R_g(M) \rangle$ scaling of the diffusion-limited aggregates (DLA) overestimates the ramification of our clusters at large M, as shown by the dash-double dotted line in section (b). The experimental data were binned for clarity of representation. The horizontal error bars denote the widths of the bins; the vertical error bars denote the standard deviation from the mean for each of the bins. For large M, there was only one cluster per bin, such that the standard deviation was not defined.

of the smallest lattice animals, which are exactly known,[19] perfectly match our experimental data at small M, as shown by the dash-dotted curve in Fig. 2(b). The $\langle R_g(M) \rangle$ scaling of the lattice animals at large M is universal for all possible two-dimensional lattice structures, regardless of their symmetry. This suggests that this simple model may possibly be used to describe our experimental clusters, which are amorphous, such that the particle positions do not in general match the symmetry of any periodic lattice.

The number of different configurations of M connected particles on a lattice, or lattice animals, is large, increasing with M. In the mathematical model of lattice animals, all types of shapes are equivalent.[1,18] However, in our experimental system, clusters of the same mass, which have different shapes, occur with different probabilities. To match the behavior of mathematical lattice animals with that of our experimental clusters, the probability for a cluster of a given mass and shape must decay as $(1-p)^L$ with its interfacial perimeter length L, where $p < 1$ is the probability for an additional particle to contact this given cluster at a certain position along the interface. For hard particles, randomly distributed on a lattice, p is simply the area fraction η of the particles. For the experimental particles, which are not restricted to reside on discrete lattice sites, we assume $p(\eta) = \omega\eta$, where ω is an unknown parameter. Thus, for a given M, the theoretical average radius of gyration of the clusters is obtained as:

$$\langle R_g(M) \rangle = \left[\sum_i (1-p)^{L_i} \right]^{-1} \sum_i R_g^i (1-p)^{L_i}, \qquad (1)$$

where the summation is carried out over all possible shapes of lattice animals of mass M, each weighted by the probability, which is attributed to its interfacial perimeter length L_i. Note, eqn (1) is commonly used to describe the clusters which appear in the theoretical percolation model.[1]

To evaluate $\langle R_g(M) \rangle$, we simulate a representative set of 10^6 random lattice animals employing an algorithm that is based on a random walk on a two-dimensional hexagonal lattice. For each of these lattice animals, the radius of gyration R_g^i and the perimeter length L_i are plugged into eqn (1), which then yields the average R_g for each M. We generate a random lattice animal of M particles in M steps. First, we pick the cell at the (0,0) position to be part of our lattice animal. Then, in each of the $(M-1)$ steps remaining, one of the cells that are NNs to the current position is chosen at random. If this cell is already part of our lattice animal, we adopt the position of this cell to be our current position and continue to the next step, without having this step counted. If the cell is not a part of our lattice animal yet, we add it to our lattice animal, adopt the position of this cell to be our current position, count this step, and proceed to the next step. An example of our generated lattice animal is shown in the inset to Fig. 2(a). For each lattice animal formed, we calculate its radius of gyration R_g^i and interfacial length L_i, which allows us to test the algorithm by comparing the average $\langle R_g \rangle$ with the known[18] scaling of the large lattice animals $\langle R_g \rangle \sim M^{0.64}$. In addition, we test the most compact lattice animals obtained by simulation as these represent a usual (2D) solid, such that $\langle R_g \rangle \sim M^{1/2}$. Unfortunately, while our simple algorithm works well in three dimensions[22] it is not as accurate in two dimensions, such that the most compact clusters scale as $M^{1/2-\nu}$, where $\nu \approx 0.03$. Once a set of 10^6 lattice animals is generated, we evaluate eqn (1) for different values of p and divide the resulting $\langle R_g(M) \rangle$ by $M^{-\nu}$ to account for the deficiencies of our algorithm. The p value is then tuned to have the theoretical $\langle R_g(M) \rangle$ perfectly fit the experimental data, as shown Fig. 2(a) (solid line).

When particles are sticky, forming permanent clusters, the probability p for an extra particle contact along the interfacial boundary depends on both η and the probability for two NNs to stick together, which is itself related to the fraction of PHSA monolayer remaining on the surface of each of these particles after etching; thus, p is now a function of both η and c. With our model we avoid the detailed modelling of interparticle interactions; instead, as in the case of the repulsive particles, we set p as a free fitting parameter. Again, a perfect match is obtained between this simple theoretical model, as shown in Fig. 2(b) (solid line), and the experimental data (scatter) with only one free parameter being used; importantly, the fitted p is different in

Fig. 2(b) and in Fig. 2(a). This perfect agreement between our very simple theoretical lattice model and the experimental data is encouraging; it suggests that, for a given η and c, the clusters may possibly be fully described by a single parameter p, which accounts for both the permanent and temporary contacts between the particles. Importantly, the $\langle R_g(M)\rangle$ data alone, with the probability for a cluster of mass M to form still unknown, do not fully characterize the 'typical' clusters in our system. Clusters of certain masses may be extremely rare, in which case their influence on mechanical or electronic properties of the macroscopic system is negligible, regardless of their shape.

3.3 Size distributions of the clusters: hard particles

To complement the statistical description of the clusters of repulsive particles, we measure the probability for a cluster of mass M to form in the system. Naïvely, the formation of a cluster may be considered a sequence of independent single-particle contact formation events, each having a certain probability s. However, the experimental size distribution $P(M)$ of the clusters is a power law $P(M) \propto M^{-\alpha}$ with a constant α (for a given η) rather than a Poisson distribution, as shown in Fig. 3, where the experimental data are plotted on a log–log scale for a system of repulsive particles. The $P(M)$ at $\eta = 0.49$ exhibit slight deviations from a power law, which becomes exponentially truncated $P(M) \propto M^{-\alpha}e^{-M/M_t}$, with M_t being a constant. The data at $\eta = 0.23$ reveal a similar, albeit much smaller, truncation. Importantly, while the data are better fitted by a truncated power law, the α index does not significantly change when the truncation exponent is either introduced or excluded from the fitting formula.

The average distance between the particles r_a scales as $\rho^{-1/2}$, where $\rho = (4\eta/\pi\sigma^2)$ is the number density of the colloids. Therefore, large clusters become increasingly probable at high densities, such that the power law index α decreases with the area fraction η.

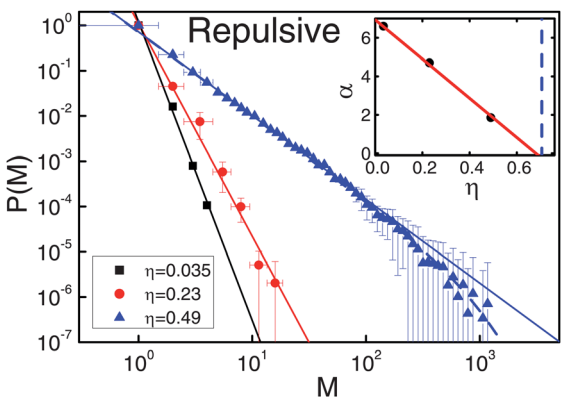

Fig. 3 The cluster size distributions $P(M)$ at several different densities η of repulsive colloids (see legend) exhibit a power law decay $P(M) \propto M^{-\alpha}$. All data are normalized $P(1) = 1$ to simplify the comparison between different η. The high η data were log-binned (the horizontal error bars indicate the bin dimensions); the vertical error bar is the standard deviation of $P(M)$ within this bin size. Slight deviation from a power law, caused by truncation by exponential decay, is observed for $\eta = 0.49$ (triangles) at $M < 200$. Interestingly, α, the power law indices of our data are linear in η (as shown in the inset), such that the extrapolation of $\alpha(\eta)$ hits zero at the melting area fraction of hard disks,[20,21] where $\eta = 0.706$ (vertical dashes).

Interestingly, the observed decrease of α with η is linear, as shown in the inset to Fig. 3. Moreover, the linear extrapolation of our experimental $\alpha(\eta)$ values hits zero at $\eta \approx 0.7$, which is very close to $\eta = 0.706$ (vertical dashes in the inset to Fig. 3), where an ordering phase transition was suggested to occur in a two-dimensional system of hard disks.[20,21] The extrapolated vanishing of α may possibly indicate that clusters of all masses are equally probable at $\eta = 0.7$. This situation is somewhat reminiscent of the critical point in a liquid[1] where the surface tension is zero and droplets of all shapes form. Clearly, the suggested scenario is highly speculative, and much more experimental and theoretical work is needed to fully establish whether this scenario is correct and how exactly the proliferation of non-crystalline clusters may be related to the onset of crystallinity at $\eta = 0.706$. If indeed a connection exists between the phase diagram of the system and the size distribution of the clusters, this further supports our conclusion that the formation of clusters can not be described as a sequence of independent contact-formation events involving uncorrelated particles; rather, the correlations between particles play an important role in cluster formation.

To further understand the physics of cluster formation, we attempt to reproduce our $P(M)$, employing the same simple lattice model, which correctly describes our experimental $\langle R_g(M)\rangle$. We fill a 100 × 100 hexagonal lattice with particles at random, such that the fraction of filled sites is η; this corresponds to the well-known percolation model.[1] For $\eta > 0.5$, a percolating macroscopic cluster spans through the system;[23] this η is known as the percolation threshold $\eta_c = 0.5$. The correlation length ξ diverges[24] at $\eta = \eta_c$, such that the theoretical $P(M)$ exhibits a power law scaling[1] M^{-2}; this power law is identical, within error, to the scaling of our experimental data at $\eta = 0.49$. However, for a smaller area fraction $\eta = 0.23$, the theoretical prediction,[25] shown in Fig. 4 (open symbols), is functionally different from the experiment (red filled circles, Fig. 4). This theoretical model predicts a relatively short ξ far from η_c, such that $P(M)$ is exponentially truncated for clusters exceeding the size ξ. The experimental $P(M)$ is much closer to a power law, which indicates that the ξ value is higher than theoretically predicted. More importantly, the experimental scaling index α, as shown in the inset to Fig. 3, is much higher than its theoretically

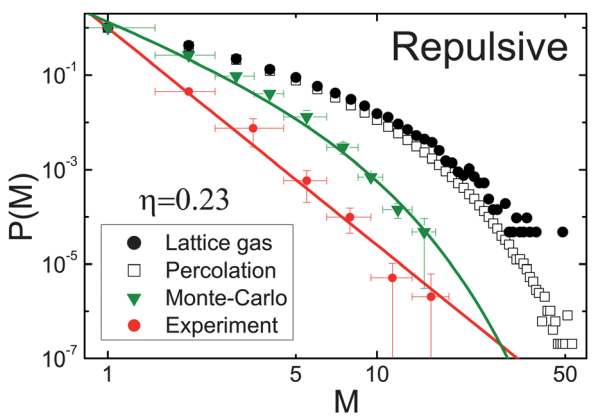

Fig. 4 Our experimental $P(M)$, obtained for the repulsive colloids at $\eta = 0.23$, exhibit a power law scaling $M^{-\alpha}$, where $\alpha \approx 4.7$, with a possible slight exponential truncation. The theoretical predictions, obtained with three different models, dramatically miss the experimental scaling.

predicted value. The failure of this very simple theoretical model is hardly surprising, since in this model the particles and the clusters do not move once deposited onto a lattice; thus, particles that are initially deposited at a distance never directly interact. This limitation of our theoretical model may possibly diminish the correlations, giving rise to the observed disagreement with the experimental $P(M)$.

To improve the agreement of our model with the experiment, we allow the particles to move randomly, after their deposition. Each particle moves in its turn to the next lattice site, in a direction that is randomly chosen for each step; this occurs as long as the chosen lattice site is vacant. If the chosen lattice site is full, the particle stays in place, waiting for its next turn to move. Somewhat surprisingly, this lattice–gas (LG) simulation is even further away from the experimental $P(M)$; while the correlation length is roughly the same as with the immobile particles, the α index is far too small, as shown in Fig. 4 (black solid symbols). Typically, the lattice models provide a reasonable approximation for the behavior of real-life systems, in which particle positions are not discretized. However, in our case, the agreement is very poor, which suggests that a continuum model may be necessary to better describe our clusters.

To overcome the limitations due to a discrete lattice, we adopt a model of simple hard disks, in which particle positions can change continuously. This model, implemented *via* direct Monte-Carlo (MC) simulations,[26] is usually capable of mimicking the behavior of the experimental colloids more closely. Our disks, of diameter σ, move on a square of size 84×84 (in σ units) subject to cyclic boundary conditions. The area fraction of the particles is $\eta = 0.23$, as in the experiment. In each step, one particle is chosen at random; this particle is moved a distance of 3.3σ in a randomly-chosen direction, on condition that the new position of this particle does not overlap with any other particle in the system. Varying the step size by a factor of 10 does not alter the results of our simulation, but may significantly increase the equilibration time. If the move of the particle results in an overlap, the move is cancelled, such that the particle remains in its original position. This process continues until the number of successful moves is $5N$, N being the total number of particles in the system, such that any dependence on the initial configuration is removed; this algorithm is the classical MC, tested over the last few decades on hundreds of different model systems.[26] Strikingly, this model, in which particle positions are continuous, is still incapable of yielding the correct functional shape for the $P(M)$ at $\eta = 0.23$, as shown in Fig. 4 (green triangles). The $P(M)$ obtained with these MC simulations are closer to the experimental data than the predictions of our lattice models. However, the power law scaling index α is still totally missed, and the correlation length is still lower than experimentally detected, as demonstrated by the higher curvature of the theoretical $P(M)$ in Fig. 4. Importantly, while slightly longer interactions than those between theoretical hard disks may be present in our experimental system, such interactions are usually taken into account by simply rescaling the particle size $\sigma_{\mathrm{eff}} = \mathrm{A}\sigma$, where A is a constant; then, the effective area fraction is $\eta_{\mathrm{eff}} = \mathrm{A}^2\eta$. This rescaled η_{eff} may be closer to η_c, where ξ is longer, such that the theoretical $P(M)$ would then scale as a power law. However, this rescaling can not bridge the disparity between theory and experiment with respect to the value of the scaling index α; the experimental $\alpha \approx 4.7$ at $\eta = 0.23$ can not be reconciled with the theoretical $\alpha \approx 2$ observed near η_c. Thus, the observed disparity is insensitive to the details of the interaction potential which suggests that a more fundamental issue may be missing in our understanding of the collective behavior in this very simple system.

3.4 Size distributions of the clusters: sticky particles

We further test the universality of our conclusions by measuring the experimental $P(M)$ with sticky, rather than repulsive, colloids. This drastic change in interparticle interactions significantly changes the nature of our clusters; instead of short-lived clusters of repulsive particles, which deform and reorganize on the scale of the particle self-diffusion time $\sim$10 s, the sticky particles form permanent clusters which have a finite elastic modulus.[5] Interestingly, while the attractive interactions in our system are irreversible, the clusters do not grow indefinitely; instead, our cluster size distribution $P(M)$ is stable on a timescale of at least two weeks. This timescale is longer, by many orders of magnitude, than the self-diffusion time of an individual particle or cluster. A similar behavior was observed earlier in a three-dimensional colloidal suspension, where cluster formation was induced by depletion interactions[4] and the $P(M)$ did not exhibit a power law.[5] However, the physical mechanism for this behavior is still not fully understood, even on a qualitative level.

Strikingly, the $P(M)$ of our permanent clusters of sticky particles scales as a power law, much like the $P(M)$ of the short-lived clusters in the repulsive system. In both cases, the $P(M)$ is subject to only slight exponential truncation, as we demonstrate in Fig. 5. The scaling index α depends, for the sticky particles, on both η and the fraction of the steric PHSA monolayer removed from the particles' surfaces. This fraction itself scales with the sodium methoxide concentration c in the etching solution as indicated in the legend to Fig. 5. Particles that were etched in a more concentrated solution have a larger fraction of their PHSA monolayer removed; these particles then have a higher chance of sticking together. The $P(M)$ for the repulsive particles, extrapolated to the same η, is also shown in Fig. 5 (green solid line) for the sake of comparison. Unsurprisingly, the probability

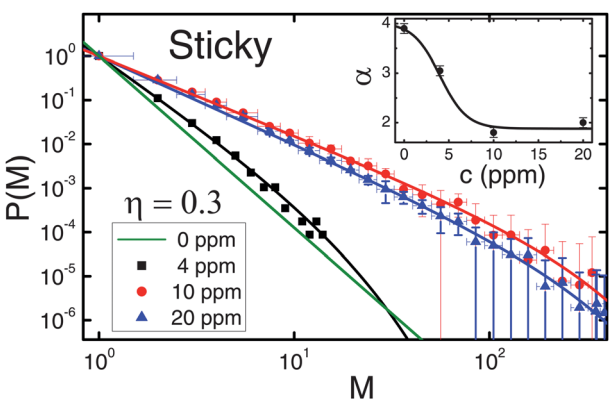

Fig. 5 The $P(M)$ of sticky colloids scale as $M^{-\alpha}$, where α depends on the concentration of sodium methoxide in the etching solution, as shown in the inset. The curved lines are the fitted power law dependencies, slightly truncated by an exponential.

for large clusters is reduced when particles are not sticky. Interestingly, the scaling index α initially decreases with c, then saturates for $c > 10$ ppm, as shown in the inset to Fig. 5. This variation of α with c is reminiscent of the $\alpha(\eta)$ variation observed in the repulsive systems. Clearly, the variation of $P(M)$ with c indicates that our particles do not undergo a diffusion-limited aggregation (DLA), where for each close approach between particles (or clusters) a permanent contact between them is ultimately established. This further supports our theoretical model in Fig. 2(b), in which the probability for contact formation is a function of c and η. Indeed, the $\langle R_g(M)\rangle$ of the DLA clusters, embedded in a two-dimensional space, scale[27] as $M^{0.583}$; this scaling does not match our experimental data, as shown in Fig. 2(b) (yellow dash-dotted line). A peaked $P(M)$, rather than a monotonically decaying power law, was predicted[28] to describe a system of DLA clusters undergoing Brownian motion in 2D at all intermediate times. A somewhat unphysical model of DLA, in which the mobility of clusters was assumed to be mass-independent,[29] yields a power law $P(M)$ with $\alpha = 0.75$. This value of α can possibly be settled with our data where α decreases with c. For even higher values of c, at the DLA limit, α may be lower than measured in our work. Our α value can also be compared to early TEM measurements, where $\alpha = 1.5$ was observed for a reaction-limited aggregation.[30] Finally, the theoretical models for cluster distributions in thermodynamically-equilibrated systems, discussed above, predict α to be invariant with the distance, in the phase space, from the percolation threshold. Only the correlation length is expected to vary, decreasing far from the percolation threshold, such that the M range, in which the power law behavior is observed, is shortened. The observed variation of α with η and c suggests that a line of critical points may exist, such that each of these points corresponds to a different value of α. This is further supported by the experimental correlation lengths, which are systematically longer than those predicted by the theory. These excessively long correlations are difficult to justify if the behavior of our system is determined by a single critical point at the percolation threshold.[31,32] While these results suggest that a line of critical points may exist, the nature of these multiple critical points is still not clear.

4. Conclusions

In conclusion, our experimental $\langle R_g(M)\rangle$, describing the shape of clusters composed of either repulsive or sticky colloids, are well-described by a simple lattice model. This is so in spite of their rather complex scaling with M, where the usual $M^{0.5}$ scaling law is observed at high M, while the smaller clusters are more ramified. The size distributions of these clusters exhibit a power law scaling, with the scaling index α being dependent on both η, the area fraction of the particles, and the parameter c, describing their stickiness. This η- and c- dependent, power law scaling, exponentially truncated at a very high M, cannot be described by the common theoretical models, such as the percolation on a lattice, the lattice–gas, and the MC simulation of hard disks. Thus, our simple and fundamental 2D system is still not fully understood, deserving further theoretical attention.

Acknowledgements

We thank Dr P. J. Lu for sharing his PLuTARC codes. We thank Prof. D. A. Weitz, Dr P. J. Lu, Prof. N. Shnerb, Prof. Y. Rabin, Dr P. Pfleiderer, Prof. J. Vermant, Dr O. Farago, and Mr A. Cohen for fruitful discussions. We thank our copy editor, Ms L. Vaks, for polishing the manuscript. This research is generously supported by the Kahn Foundation and the Israel Science Foundation (#85/10, #1668/10).

References

1 D. Stauffer, *Phys. Rep.*, 1979, **54**, 1–73.
2 A. Moncho-Jordá, A. A. Louis and J. T. Padding, *Phys. Rev. Lett.*, 2010, **104**, 068301.
3 A. Jarosik, U. Traub, J. Maier and A. Bunde, *Phys. Chem. Chem. Phys.*, 2011, **13**, 2663–2666.
4 P. J. Lu, J. C. Conrad, H. M. Wyss, A. B. Schofield and D. A. Weitz, *Phys. Rev. Lett.*, 2006, **96**, 028306.
5 P. J. Lu, E. Zaccarelli, F. Ciulla, A. B. Schofield, F. Sciortino and D. A. Weitz, *Nature*, 2008, **453**, 499–503.
6 J. D. Stevenson, J. Schmalian and P. G. Wolynes, *Nat. Phys.*, 2006, **2**, 268–274.
7 R. Pecora, *Dynamic light scattering*, Plenum Press, New York, USA, 1985.
8 J. R. Savage and A. D. Dinsmore, *Phys. Rev. Lett.*, 2009, **102**, 198302.
9 Y. Peng, Z. Wang, A. M. Alsayed, A. G. Yodh and Y. Han, *Phys. Rev. Lett.*, 2010, **104**, 205703.
10 A. Yethiraj and A. van Blaaderen, *Nature*, 2003, **421**, 513–517.
11 R. P. A. Dullens, *Soft Matter*, 2006, **2**, 805–810.
12 A. Yethiraj, *Soft Matter*, 2007, **3**, 1099–1115.
13 Z. Zhang, P. Pfleiderer, A. B. Schofield, C. Clasen and J. Vermant, *J. Am. Chem. Soc.*, 2011, **133**, 392–395.
14 L. Xu, A. Berges, P. J. Lu, A. Studart, H. Oki, A. B. Schofield, S. Davis and D. A. Weitz, *Phys. Rev. Lett.*, 2010, **104**, 128303.
15 P. J. Lu, P. A. Sims, H. Oki, J. B. Macarthur and D. A. Weitz, *Opt. Express*, 2007, **15**, 8702–8712.
16 J. C. Crocker and D. G. Grier, *J. Colloid Interface Sci.*, 1996, **179**, 298–310.
17 G. Ambrosetti, I. Balberg and C. Grimaldi, *Phys. Rev. B: Condens. Matter Mater. Phys.*, 2010, **82**, 134201.
18 H. P. Hsu, W. Nadler and P. Grassberger, *J. Phys. A: Math. Gen.*, 2005, **38**, 775–806.
19 I. Jensen, *J. Stat. Phys.*, 2001, **102**, 865–881.
20 K. Binder, S. Sengupta and P. Nielaba, *J. Phys.: Condens. Matter*, 2002, **14**, 2323–2334.
21 Z. Wang, W. Qi, Y. Peng, A. M. Alsayed, Y. Chen, P. Tong and Y. Han, *J. Chem. Phys.*, 2011, **134**, 034506.
22 E. Sloutskin, P. J. Lu, T. Kanai, and D. A. Weitz, in preparation.
23 S. Galam and A. Mauger, *Phys. Rev. E: Stat. Phys., Plasmas, Fluids, Relat. Interdiscip. Top.*, 1997, **56**, 322–325.
24 G. D. Quinn, G. H. Bishop and R. J. Harrison, *J. Phys. A: Math. Gen.*, 1976, **9**, L9–14.
25 We test our simulations by a comparison to the analytical $P(M)$[33].
26 D. Frenkel and B. Smit, *Understanding molecular simulation: from algorithms to applications*, 2nd edn, Academic Press, San Diego, USA, 2001.
27 H. E. Stanley, *Fractals and multifractals: the interplay of physics and geometry*, in *Fractals and disordered systems*, ed. A. Bunde and S. Havlin, Springer-Verlag, Berlin, Germany, 1991.
28 P. Meakin, T. Vicsek and F. Family, *Phys. Rev. B*, 1985, **31**, 564–569.
29 T. Vicsek and F. Family, *Phys. Rev. Lett.*, 1984, **52**, 1669–1672.
30 D. A. Weitz and M. Y. Lin, *Phys. Rev. Lett.*, 1986, **57**, 2037–2040.
31 J. H. Ke, Z. Q. Lin and X. S. Chen, *Chin. Phys. Lett.*, 2009, **26**, 058201.
32 G. L. Olson, *Ann. Nucl. Energy*, 2008, **35**, 2150–2155.
33 M. F. Sykes and M. Glen, *J. Phys. A: Math. Gen.*, 1976, **9**, 87–95.